Master's Thesis of Engineering

Design of Pneumatic Wearable Devices for Arm and Hand Rehabilitation

팔과 손의 재활을 도울 수 있는 공압 웨어러블 디바이스 개발

February 2020

Graduate School of Engineering
Seoul National University
Mechanical Engineering Major

Sehun Park

팔과 손의 재활을 도울 수 있는 공압 웨어러블 디바이스 개발

Design of Pneumatic Wearable Devices for Arm and Hand Rehabilitation

Advisor Yong-Lae Park

Submitting a master's thesis of Public Administration
October 2019

Graduate School of Engineering
Seoul National University
Mechanical Engineering Major

Sehun Park

Confirming the master's thesis written by
Sehun Park
December 2019

Chair Kunwoo Lee (Seal)

Vice Chair Yong-Lae Park (Seal)

Examiner Sung-Hoon Ahn (Seal)

Abstract

Arm and hand disabilities can result from a number of diseases or injuries. Patients particularly with arm and hand disabilities have difficulty in daily activities while follow-up care and rehabilitation are critical to recovery of the patients in this case. However, they have to make personal trips to clinics or hospitals for follow-up treatments since most of existing devices available are bulky, heavy and even expensive in general, discouraging the patients from having them home. This paper proposes inflatable wearable devices for rehabilitation with bio-inspired design. Since the main actuation mechanism is pneumatic inflation, the devices are lightweight, safe, and affordable compared to conventional devices. When the actuator of the device is inflated, the actuator can assist hand or forearm motion depending on where the actuator is placed. The proposed rehabilitation devices, which can be conjointly used with typical clothing materials, provide comfort for the user by easily conforming the three-dimensional geometries of the forearm and hand. To characterize the system, the angle and the assist torque of the joint were measured while operating the device with arm and finger models. For arm and hand wearable devices, results of feasibility tests were also presented.

Keyword: Soft Robotics, Artificial Muscle, Wearable Device, Rehabilitation Robot

Student Number: 2017-26770

Table of Contents

Chapter 1. Introduction

Arm and hand disabilities are often caused by stroke, fractures and incised/punctured injuries. Having a cup of water and wearing clothes may no longer be simple daily tasks for patients with arm and hand disabilities [1]. In order to help the patients return to their daily lives, it is well known that follow-up care is critical [2], [3]. We propose lightweight, soft wearable devices for forearm and hand rehabilitation (Fig. 1 and 2). Among several rehabilitation processes, robot-assisted arm training is widely used these days and improves patients' motor function effectively [4], [5], [6]. A general mechanism of existing robotic rehabilitation is that a robot exerts assistive/resistive forces to help the patient recover function of the forearm muscles while the patient is holding the handle of the robotic device [7], [8], [9].

Traditional devices for robot-assisted rehabilitation are mostly made of rigid materials, making the devices costly, stationary, and heavy [10], [11], [12]. Since these characteristics can hamper subsequent treatments of the patient, there is a compelling need of devices made of soft materials (e.g. polymer or fabric). With the advantages of i) compliance to unstructured geometries (e.g. curved surfaces), ii) reduced chances of injuries in case of malfunctioning, iii) cost efficiency, and iv) lightweight and compact form factor, there have already been approaches of building orthotic devices for rehabilitation using soft materials: a soft tendon-driven

glove made of silicone for assisting flexion and extension motions of patients with hand paralysis [13], A bio-inspired soft wearable robotic device that can help patients recover from neuromuscular diseases by assisting dorsiflexion and plantarflexion of the ankle joint [14], and a wearable assistive robotic device made of bellow actuators for elbow rehabilitation [15].

However, a soft robotic device that assists wrist motions of pronation/supination has not been much investigated yet. A helical actuator made of silicone and fabric was recently developed to assist pronation and supination motions of the forearm [16]. However, this silicone type actuator needs high pressure to inflate silicone bladder leading to a safety issue. Another wearable device for assisting pronation and supination uses McKibben artificial muscle actuators [17]. Since McKibben artificial muscle actuator is too bulky to be wound around the forearm, this actuator is not appropriate to be utilized to assist rotational motions. Therefore, full range of forearm rotation cannot be achieved by this device. In contrast to these actuators, flat pneumatic actuators are ideal for rotational motions of the wrist due to their near-zero initial volume. Therefore, we propose a lightweight and compact wearable device made of flat soft pneumatic actuators to assist pronation and supination motions of the wrist (Fig. 1). This device can significantly increase wearability and effectiveness of rehabilitation.

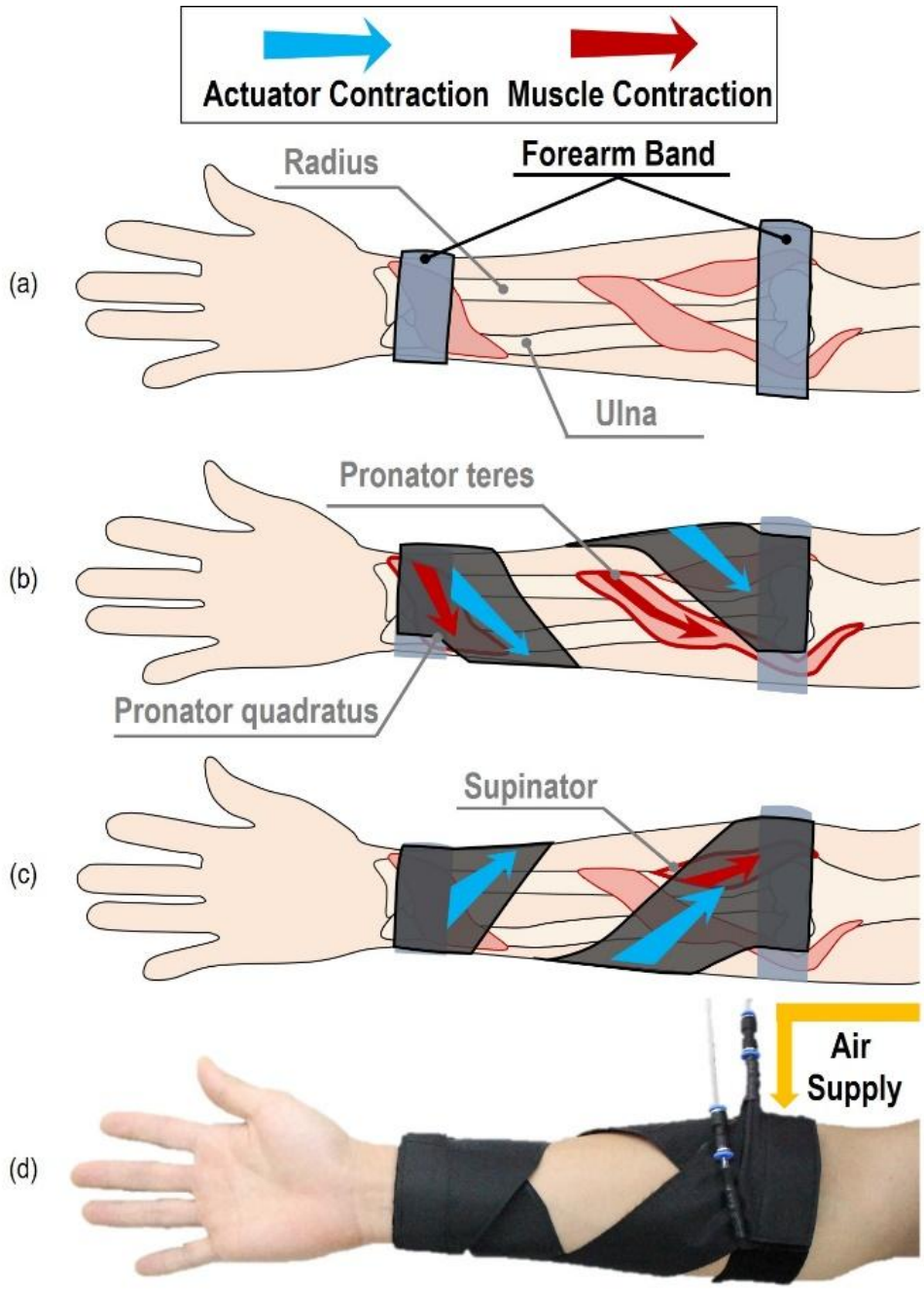

Figure. 1. Design and mechanism of the proposed wearable device for forearm rehabilitation showing (a) the arm bands for easy anchoring of the actuators, the muscles and the actuators for (b) pronation and (c) supination, and (d) an actual prototype on human arm.

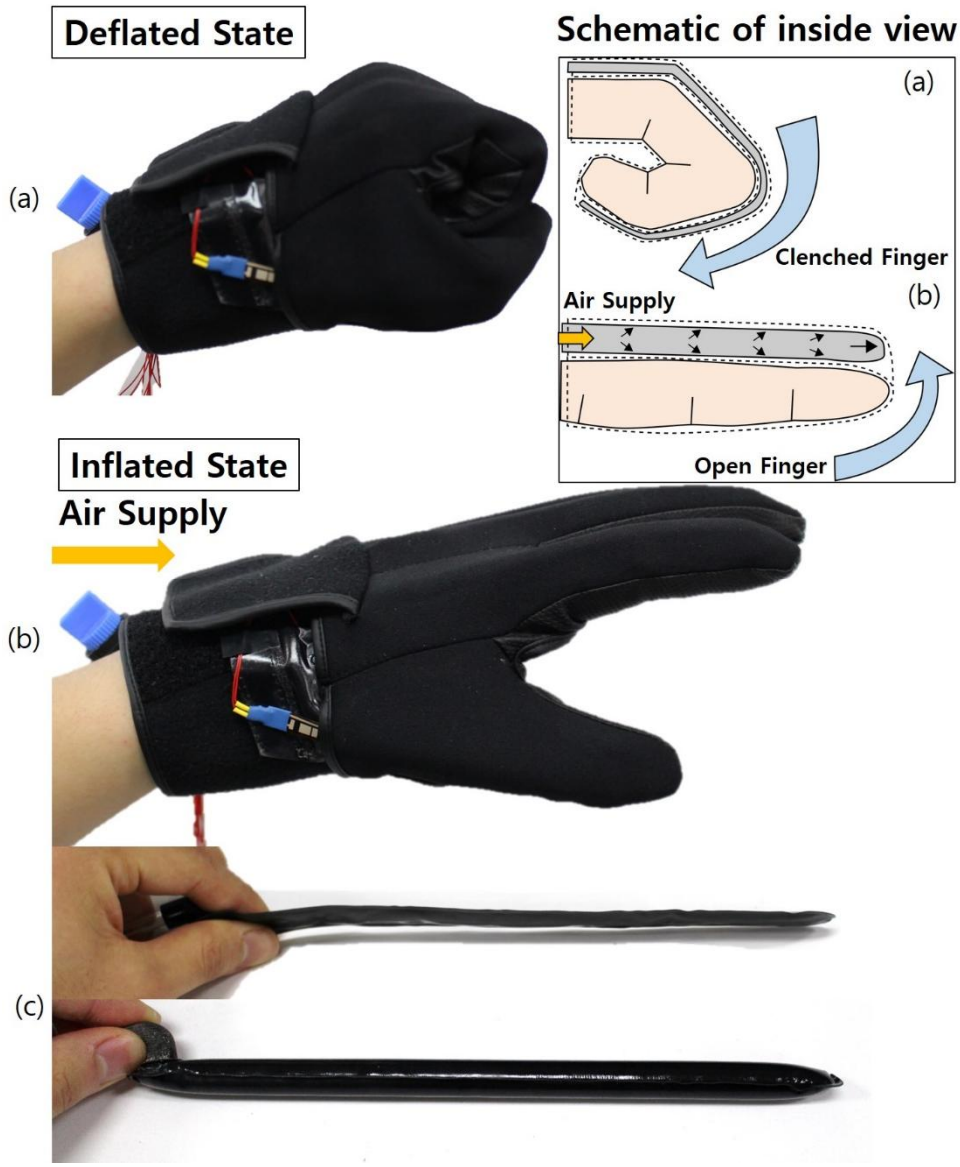

Figure. 2. Design of the proposed wearable device for hand rehabilitation device showing (a) the deflated state and (b) the inflated state with schematic of inside view, and (c) the deflated and inflated state of the actuator

We also present development of a soft glove-type device for hand rehabilitation by using the same inflatable actuator. Although the mechanism of a soft robotic glove was already proposed [18], [19], the device presented in this paper is easy to fabricate and has high wearability compared to previous devices. The device comprises inflatable actuators enclosed by a custom-designed glove (Fig. 2). This device can assist extension motion of the fingers with high compliance that make it easily wearable.

Flat pneumatic actuators are fabricated using a custom-built heat sealer with a motorized stage that can create complex sealing patterns [20]. Before fabrication of the actuators, the system was characterized to find the right parameters that ensured the robustness of the actuators.

An arm and a finger models were used for the characterization of forearm and hand rehabilitation devices. After installing the device to arm and finger models, the assist torques were measured with varied input pressures. For forearm rehabilitation device, the collected torque data were used to control the rotation angle using an optical motion sensing system. For hand rehabilitation device, the feasibility test with several subjects was conducted using the flex sensors integrated with the glove to prove that the assist torque is large enough to extend fingers.

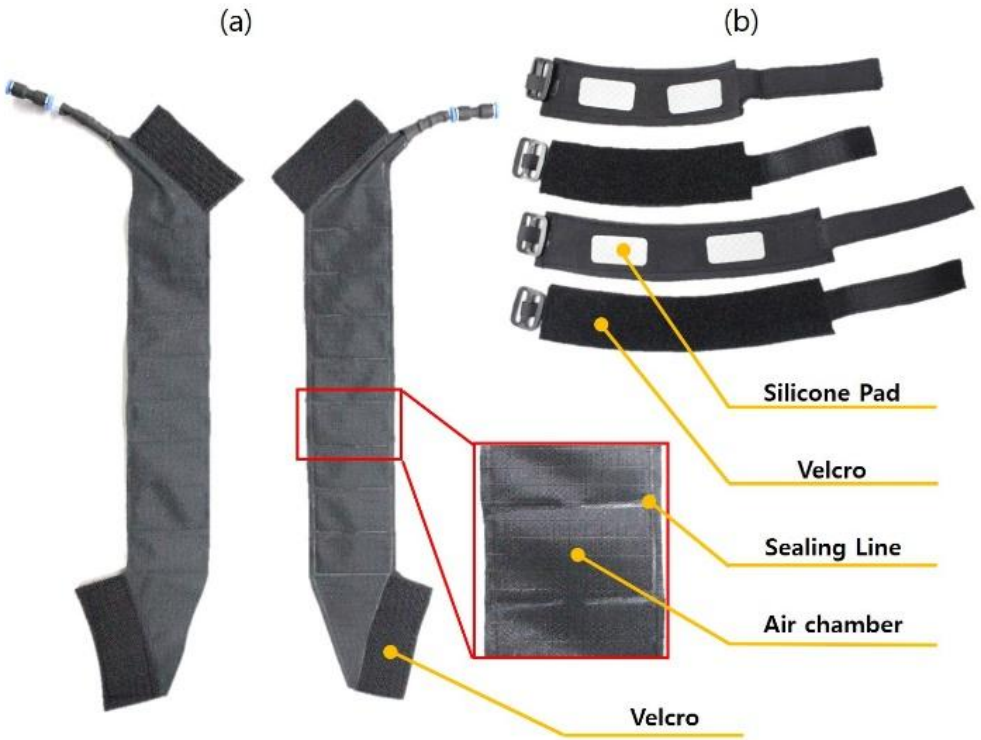

Figure. 3. (a) Flat pneumatic inflatable actuator unit with close-up of air passages and air chambers and (b) front and back views of the forearm bands.

Chapter 2. Design

2.1 Forearm rehabilitation device

2.1.1. Bio-inspired design

The design inspired by biological musculoskeletal system was based on two forearm muscles: the supinator attached to the lateral epicondyle and the radius, and the pronator teres attached to the medial epicondyle and the radius. Two actuators in an antagonist pair perform the same function of the two muscles depending on the attachment position.

The forearm bands on the upper and the lower parts of the forearm anchor the both ends of the actuators (Fig. 1). The actuator is wound around the forearm and the attachment position can be adjusted by using Velcro straps. Depending on the wound direction of the actuator, the forearm supinates or pronates when the actuator contracts.

2.1.2. Flat pneumatic inflatable actuator

While the human muscles are directly attached to rigid structures (i.e. bones) and covered with skin, the actuators have to be placed on the skin. For this reason, the proposed artificial muscles must be

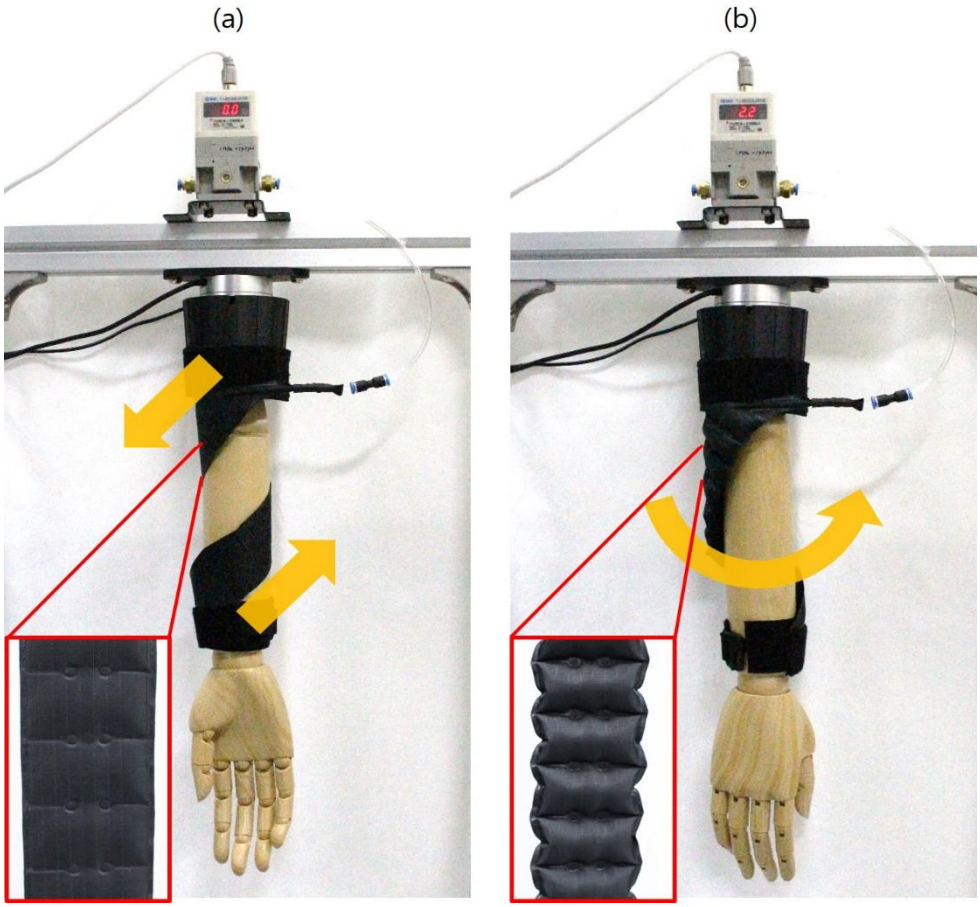

slim unlike human muscles since the compression of bulky actuators

Figure. 4. Prototype of the proposed wearable device installed on arm model showing the directions of (a) the actuator contraction and (b) the arm rotation respectively.

cause discomfort to the forearm. Therefore, the flat pneumatic actuator was chosen over McKibben muscle [21]. With the choice of actuators, the anchoring method is also very important since the skin where the actuators are attached may stretch and rotate around the bone. Fabric material was selected for actuators to

utilize various clothing techniques for increased wearability and easy fabrication.

The proposed wearable device is composed of two symmetric flat pneumatic inflatable actuator units made of heat-sealable fabric. Each actuator was fabricated using a custom-built motorized heat sealing system and has multiple air chambers connected in series. The pneumatic connections (i.e. air passages) between chambers enable simultaneous inflation (or axial contraction) of all the chambers (Fig. 3). The zero-volume air chamber becomes completely flat when deflated, which is highly useful for wearability [21]. The injection of compressed air into the air chambers makes the actuator axially contract with radial expansion like biological muscles (Fig. 4).

2.1.3. Device configuration

The range of pronation/supination of the forearm with an extended elbow position is about 160° [22]. Therefore, each actuator should have a similar range of motion. Although the contraction ratio of general pneumatic artificial muscles ranges from 10 only up to 30% [23], a relatively large rotation angle can be achieved if the length of the arm (L_f) is fixed between the two ends of the actuator. Fig. 5 shows the drawing of the flat pneumatic actuator assuming the forearm is a truncated cone. The blue area with a small radius indicates the wrist and the yellow area with a

large radius indicates the elbow. The light gray area is the flat pneumatic actuator when deflated, and the dark gray area is the actuator when inflated. The two pivot points of the actuator play a role of hinges. When the actuator contracts, the initial length of the actuator (L_i) shortens and the rotation is made until the length between the two pivot points (L_p) becomes the same as the forearm length (L_f). If the design factors, such as the contraction ratio, the arm circumference, etc. are given, any range of motion can be determined based on simple geometry calculation.

However, the force generated during the contraction of the actuator not only rotates the forearm but also pulls the forearm bands in the axial direction. As if this force increases, the forearm band may slip and hinder the operation of the actuator. In order to avoid this unwanted slip, the number of turns of the actuator has to increase so that the angle between the actuator and the forearm band becomes smaller. However, since too many turns could cause discomfort to the user, a sing turn of 360° was chosen in our prototype.

The larger the contraction ratio of the actuator is, the more the forearm rotates when the actuator has the same number of turns. To obtain a large contraction ratio, the length of the single chamber needs to be wide and long. However, the size of the single chamber also determines the entire size of the device affecting the wearability. In reference to previous research, 28mm length and 50mm width were adopted to achieve the contraction rate of 25%

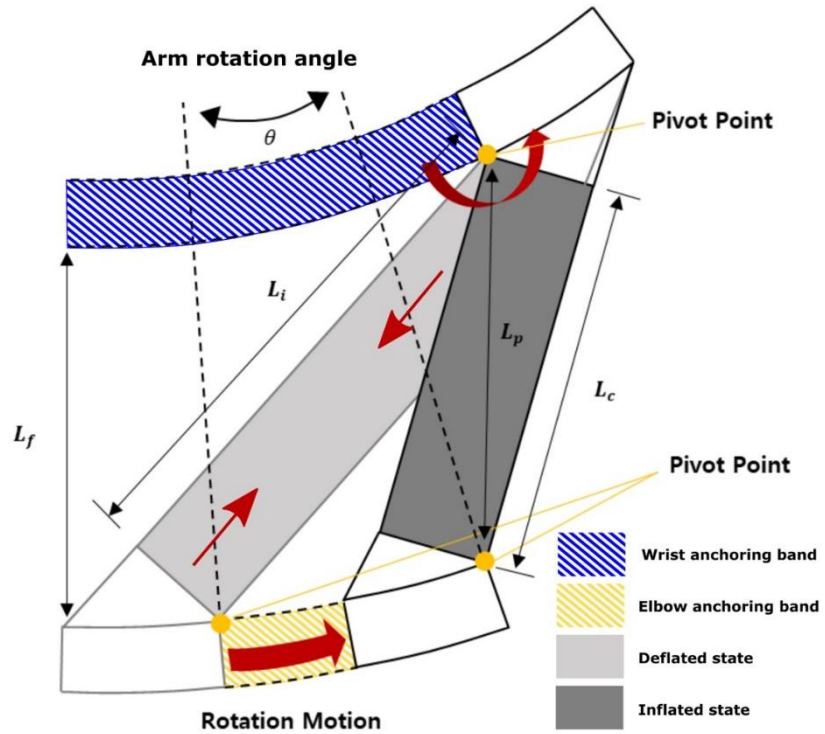

for the wearability, and nine air chambers were chosen [23].

Figure. 5. Mechanism of the actuator rotating a forearm showing the actuator before contraction (light gray area) and after contraction (dark gray area).

The forearm bands were made of double-layered fabric (Polyester 88%, Spandex 12%, 460g/yd). This fabric has high air permeability which enhances the ventilation of the device for a long-time use. Moreover, the friction force of the double-layered fabric is relatively high because the surface of the inner layer is uneven and bumpy. Anti-slip pads were also attached to the forearm bands for stable adhesion to the patient's arm when the device was actuated. Hook-and-loop fasteners and tri-glide buckles were used to fit the device to various sizes and geometries

of arms. With these features, easy wearing and removing, stability, comfort and wearability are achieved.

2.2 Hand rehabilitation device

2.2.1. Device overview

For patients with hand disabilities, rehabilitation is essential to help patients return to daily life. One of common exercises for hand rehabilitation is to grasp an object or a tool and move it [24]. Therapists need to assist patients to extend fingers before hand exercise because most patients with hand disabilities from neuromuscular diseases tend to have difficulty in opening the hand [25], [26]. However, when fingers are forced to extend by a therapist, the patients hardly feel the object leading to lack of therapeutic effect. Also, the key of rehabilitation process is the timing of the movement feedback after patients' intention to open fingers. Traditional robot-assisted hand rehabilitation devices have been made of rigid materials such as motors and linear actuators [27], [28], [29]. These devices also have limitations like kinematic compatibility with human joints, discomfort for users and safety issues. In order to overcome these problems, several types of a soft glove have been developed. For examples, a bio-inspired tendon glove has a great potential since the mechanism of winding tendon wire is the same as that of contracting actual muscles achieving under-actuated mechanism [30], [31], [32]. Pneumatic

devices have been also developed to assist hand flexion using silicone [33], [34], [35]. However, these previous devices are hard to fabricate due to tendon anchoring and silicone molding. Therefore, easy fabrication is needed to decrease cost of manufacturing rehabilitation devices.

2.2.2. Device configuration

Main parts of the device comprise a pneumatic actuator and a custom glove (Fig. 6). The pneumatic actuator has five air chambers for all five fingers, one outlet for air supply and five flex sensors (Flex Sensor, Sparkfun). Since the material of the actuator is not extensible, a flex sensor can be directly attached to the actuator. The length of each actuator is determined by the length of the corresponding finger. The length of the actuators is longer than that of the actual fingers because each actuator needs to cover not only the corresponding finger but also the joint. The widths of all the actuators are the same to be 20 mm. The custom-made glove has pockets to hold the actuators individually.

Since the lower part (close to a wrist) of the actuator is attached to the glove through Velcro, the upper part of the actuator can easily slide in the pocket of the glove even with high curvature bending. This sliding motion is necessary because the pocket of the glove can stretch following finger flexion, but the actuator is made of inextensible fabric. Moreover, the actuator can be easily replaced

in case of any failures.

Since the glove should be easily wearable by the user with disabilities, an open palm design with a wrist strap was chosen

(Fig. 6). A wrist extension strap was attached to the glove to fix the position of the wrist to assist the user for grasping. The size of each chamber is the same as that of each actuator.

Figure. 6. (a) Pneumatic inflatable actuator integrated with five flex sensors and (b) Front and (c) back views of the custom glove for patients with hand disabilities.

2.3. Power and control system

The power and control system of the proposed two devices consists of an air compressor (Bettle compressor, Sparmax), an air pressure regulator (ITV0030, SMC), a real-time data acquisition and controller board (myRIO, National Instruments), an AC/DC adaptor (APL-2402, Apower), and a wireless communication device (Xbee, Digi). The weight of the system is approximately 2.6 kg including the case and the cables (Fig. 7). The system is light enough to be installed in home. Other previously developed pneumatic wearable robots usually require high air pressure range causing a bulky power system. However, the proposed devices can generate high torque compared to other pneumatic actuators requiring relatively compact power and control system. A signal can be received using wireless communication, which can be further utilized to respond to the patients' biological signal, such as a functional near-infrared spectroscopy (fNirs), an electro-encephalogram (EEG), and electromyography (EMG).

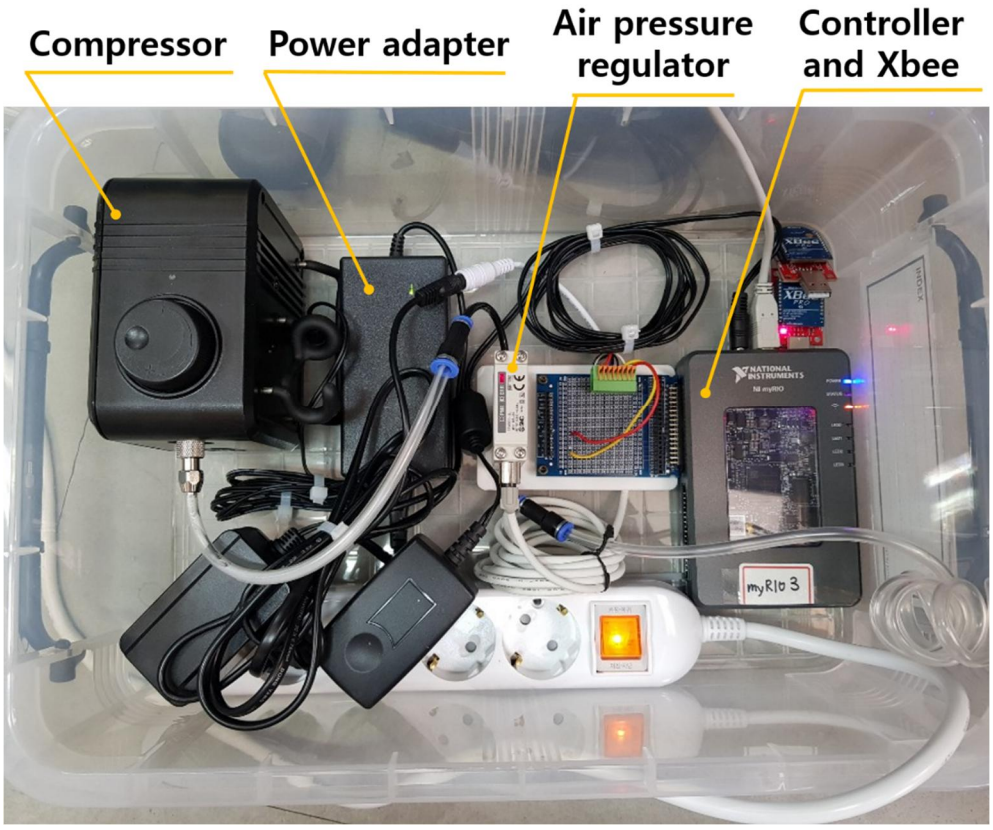

Figure. 7. The power and control system of the devices generating maximum 2.1 bar.

Chapter 3. Fabrication

3.1. Material

Both actuators of the proposed devices utilize the same fabric called heat-sealable Ripstop (Seattle Fabrics). This fabric is a composite material of Ripstop fabric and nylon, which has zero air permeability through the stitches of the fabric. The merit of Ripstop fabric is high burst strength, preventing ripping caused by frequent inflations. In addition, it can easily be integrated with other clothing materials by sewing.

3.2. Custom built heat sealing system

3.2.1. System overview

Since reliability, consistency and durability are key factors in rehabilitation devices, we decided to build an automated fabrication system for building inflatable actuators with robustness and consistency. There have been different heat sealing methods for fabricating inflatable structures, such as manual patterning, heat press, and automatic patterning [36]. Since manual sealing mostly depends on the personal skills of the operator and does not require a complicated system for sealing, it is simple and cost-effective.

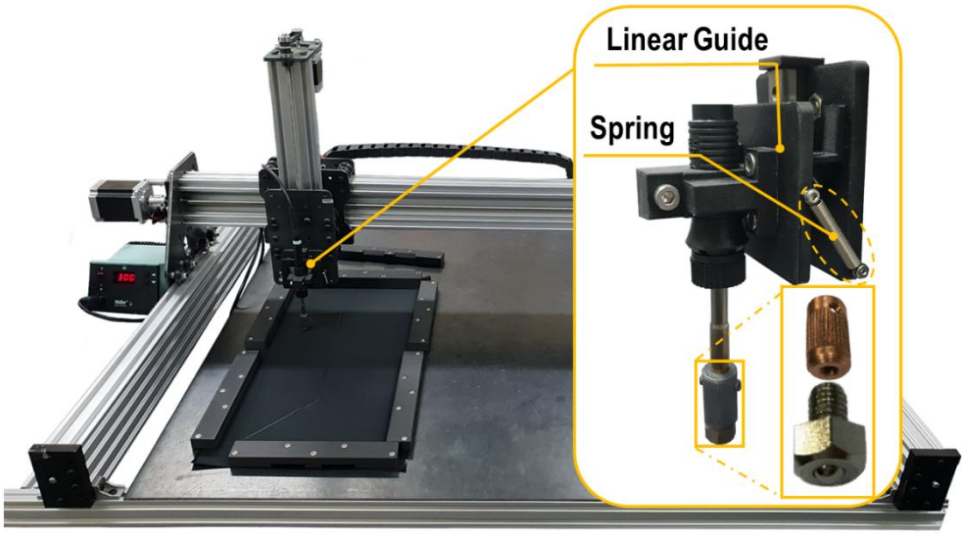

Figure. 8. Setup of motorized three-axis heat sealing stage and the expanded view of the heat application unit.

However, it is sometimes time-consuming and does not guarantee the quality of the products. Heat press is a more reliable fabrication method using thermally conductive stencils for sealing. However, it is not efficient if the sealing patterns of the product change frequently. Automatic patterning is the most effective heat sealing method for fast-paced applications compared with the other two methods. In general, a heat applicator is used as an end-effector in a motorized x-y-z stage to draw sealing patterns with simple 2D sketches. This method is also free of preparing heavy and bulky stencils. Therefore, we decided to employ automatic patterning for fabricating inflatable actuators with relatively complex patterns.

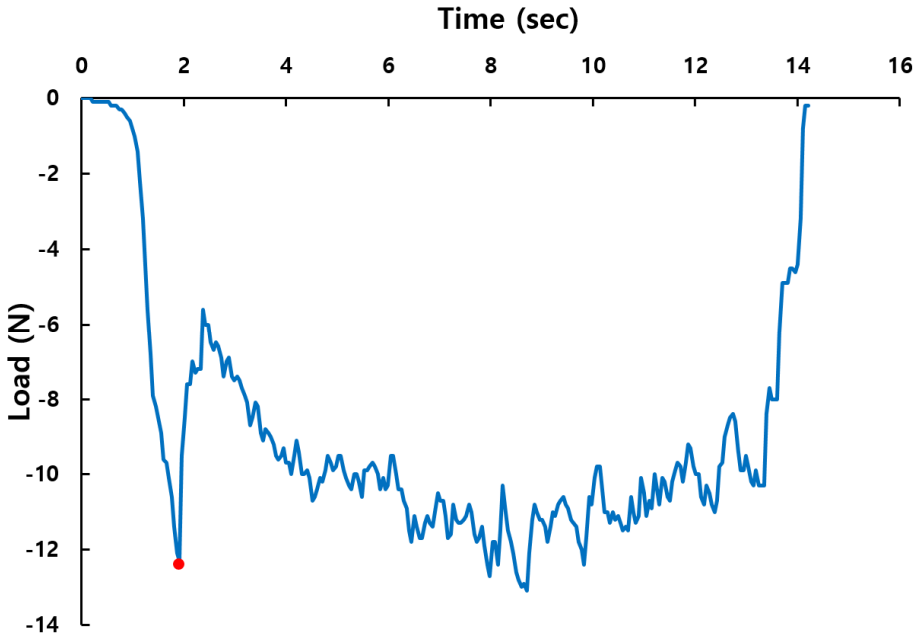

Figure. 9. Definition of the first peak of peeling test. The first peak value of the load indicates the quality characteristic value, which is the time when the inflatable actuator loses its functionality.

A soldering iron equipped with a spherical rollerball tip was mounted on a three axis motorized stage with a work space of 950 mm × 900 mm (Fig. 8). The rollerball tip with a diameter of 4.95 mm facilitates smooth movement of the end-effector by minimizing the dragging force while drawing the pattern. The position in x and y coordinates is controlled by the control unit based on the 2D sketch input. However, the z-coordinate cannot be controlled quickly when there is an unexpected vertical level change of the work space, which often happens when the base of the sealing system is not perfectly flat. While the fabrics are not

completely sealed due to the reduced vertical force of the tip on a declining plane, there is too high normal force exerted to the substrate, resulting in burnt, torn, or squashed fabrics on an inclined plane. In the worst case, it may cause permanent damage to the machine too. To address this issue, passive compliance in z-axis was provided for the sealing tip by attaching a linear guide and springs on the mounting block. The linear guide allows only the vertical movement of the end-effector and quickly react to the uneven surface. The pre-tensioned spring helps the end-effector maintain relatively constant pressure to the fabric substrate in z-axis, which enhances the robustness and the consistency of the sealing patterns.

3.2.2. Characterization

There are a few parameters that determine the quality of the sealing patterns: sealing speed, temperature of the heating element, and the initial height of the end-effector in z-axis. We used Taguchi methods to find right parameters for robustness of the actuator. The initial parameters with three levels were displayed in the $L_9(3^4)$ orthogonal array. We first made nine test samples with a 30 mm long straight line pattern to test with different parameters as listed in Table Ⅰ. Then, we conducted peeling tests with the samples with a motorized tensile test stand (Mark-10, ESM303). The first peak value of the load is determined to be the quality

characteristic value because the inflatable actuator loses its functionality once it starts leaking (Fig. 9). It means that the sealing robustness increases as the first peak load becomes larger. Thus, Taguchi's larger-the-better theorem [37] is applied to calculate the signal-to-noise (S/N) ratios shown in Eq. (1) where y_1 is the quality characteristic value and n is the test number. The experiment levels with the highest S/N ratios were selected for the second test (Fig. 11-a).

$$\frac{S}{N}\text{ratio} = 10 \cdot \log\frac{1}{n}\left(\sum_{n}^{i=1}\frac{1}{{y_i}^2}\right) \qquad (1)$$

Table Ⅱ summarizes the parameters for the second test samples. The temperature value was fixed to 350℃ because it might burn the fabric at a higher temperature. The orthogonal design was changed to $L_4(2^3)$ because there were physical limitations in other parameters. As a result of the experiments, the sealing speed, the temperature, and the z-value were determined to be 40 mm/min, 350℃, and 4.5 mm, respectively (Fig. 10-b).

TABLE I

$L_9(3^4)$ ORTHOGONAL ARRAY FOR THE FIRST TEST SET

Test Sample No.	Sealing Speed (mm/min)	Temperature (°C)	Z-value (mm)	S/N Ratio (dB)
#1	150	350	2	22.28
#2	150	300	3	13.62
#3	150	250	4	13.06
#4	100	350	3	23.75
#5	100	300	4	18.17
#6	100	250	2	10.37
#7	50	350	3	24.30
#8	50	300	2	19.28
#9	50	250	4	10.88

TABLE II

$L_4(2^3)$ ORTHOGONAL ARRAY FOR THE SECOND TEST SET

Test Sample No.	Z-value (mm)	Sealing Speed (mm/min)	S/N Ratio (dB)
#1	4	50	20.42
#2	4	40	22.92
#3	4.5	50	21.80
#4	4.5	40	24.51

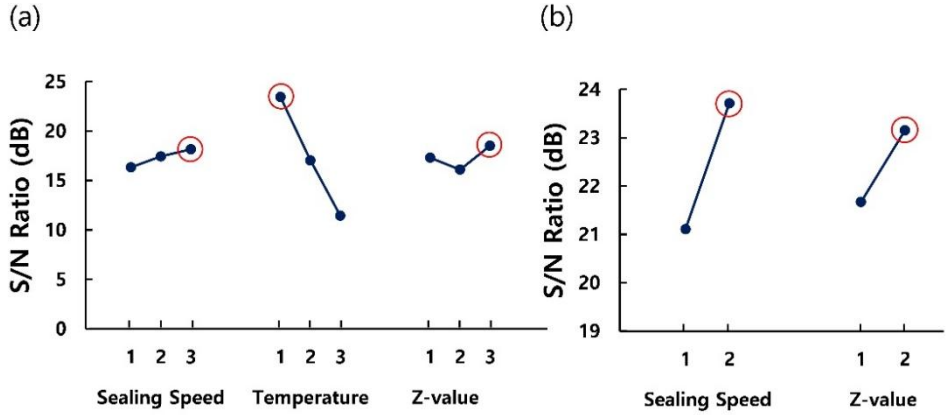

Figure. 10. S/N ratios for (a) the first test set and (b) the second test set. Red circles indicate the highest S/N ratios based on each parameter.

Chapter 4. Experiments

4.1. Forearm rehabilitation device

4.1.1. Characterization

Experiments for characterization ware conducted to obtain the relationships between the contraction force and the length of the actuator and between the forearm rotation angle and the torque of the wearable device. In the first experiment, tension between the two ends of the actuator was measured as the length of the actuator decreased under five different pressure levels (10, 20, 30, 40, and 50 kPa) with the motorized test stand (Mark-10, ESM303) (Fig. 11). The contraction force decreased as the length of the actuator shortened like other pneumatic actuators (Fig. 12).

In the second experiment, a torque sensor (RFT60-HA01, ROBOTUS) and an encoder (SME360CAP-12, SERA) were mounted on the bottom of the aluminum structure and the arm model was rotated along the axis of the encoder (Fig. 13). There was no mechanical resistance during rotation, since the arm was attached only to the axle of the encoder. After fixing the hand to the wrist holder shown in Fig. 13, the actuator was inflated and the torque was measured by the force-torque sensor at the top of the arm setup. The radius of the upper part of the arm to which the

force was applied was 4.14 cm. The z-axis torque was measured under five different pressure levels (10, 20, 30, 40, and 50 kPa) as the arm was rotated 180° with increments of 5°. The graph shows that the torque approaches to zero as the arm angle reaches 180°. Since the actuator was designed to rotate up to 180°, the result shows the approximation that the two ends of the actuator work as pivot points was reasonable (Fig. 14). However, average values of maximum pronation and supination torque in right-handed adults without disabilities are 7.5 Nm and 5.5 Nm for pronation and supination respectively [38]. Although the maximum torque of the proposed device is lower than maximum biological pronation and supination torque, this device can be expected to be used for patients with mild paralysis.

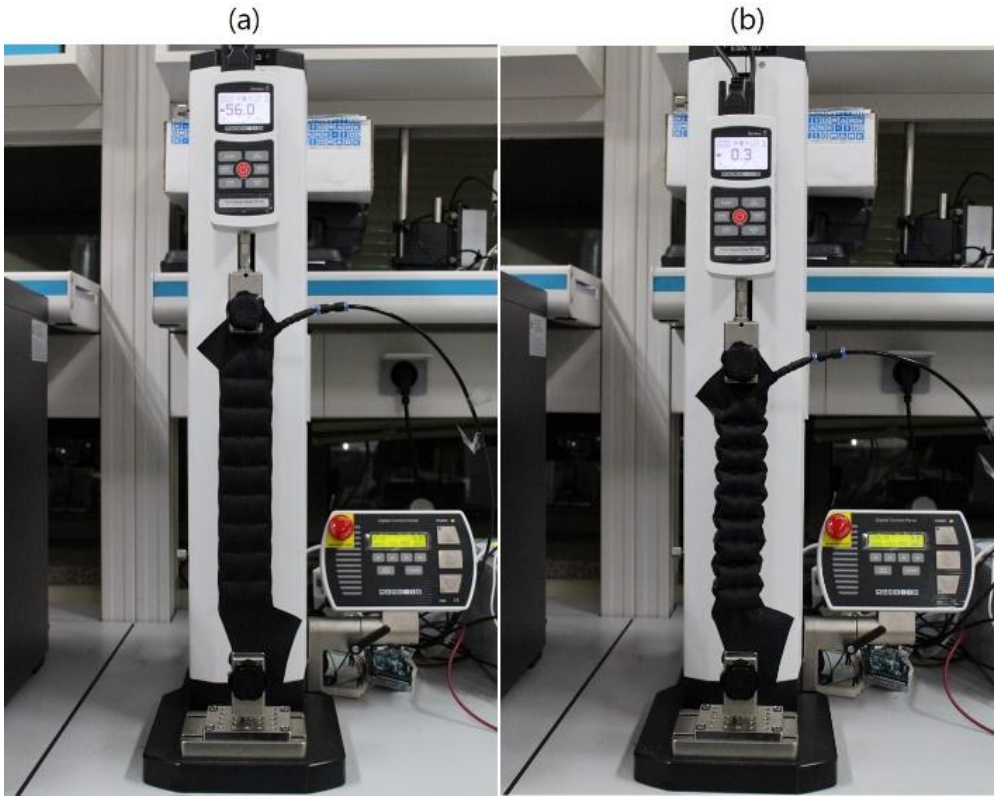

Figure. 11. Experiment setup for measuring tension and length of the actuator under different air pressures. (a) The flat pneumatic actuator with 0% contraction ratio and (b) the flat pneumatic actuator with 20% contraction ratio.

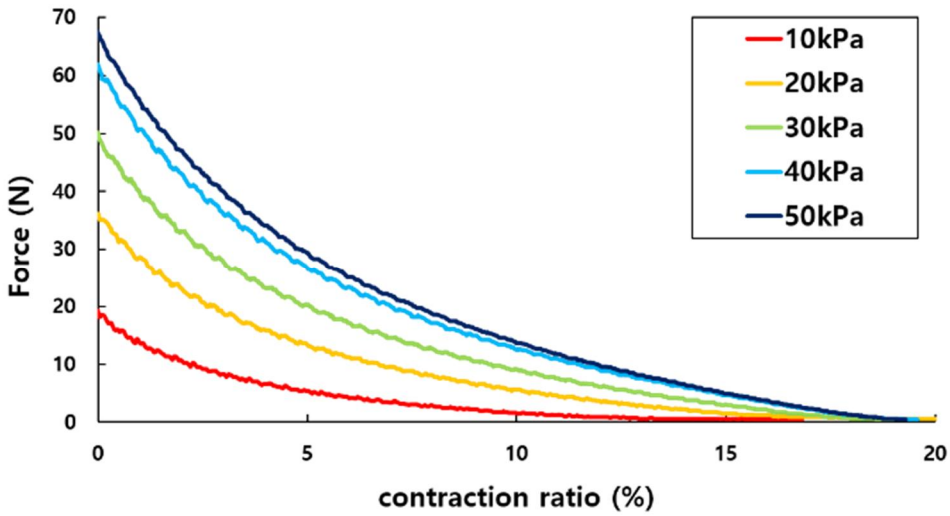

Figure. 12. Force-Length relationship of the device with different pressure levels

4.1.2. Position control with vision feedback

Position control was tested to evaluate the feasibility of helping patients rotate their forearm while they could not reach the desired positions by themselves. With the characterization results, pressures for each actuator were calculated by force equilibrium. Since the data from the characterization were discrete, linear interpolation was used. In addition to this open-loop control, the device was tested with closed-loop control, since the user's own muscles may disturb the desired motion of the device. A vision system composed of an RGB and an infrared cameras (Kinect) was set up to collect the angle changes of the forearm. MATLAB was used to process the vision data. The vision system was placed on the ground and the arm model was rotated above it (Fig. 15).

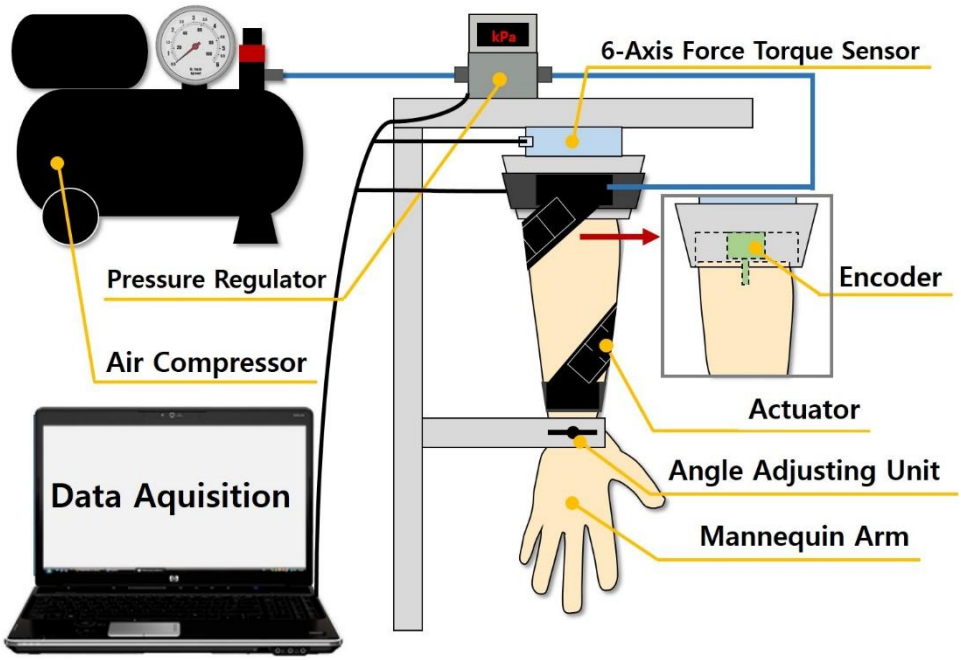

Figure. 13. Experimental setup for characterization of the device

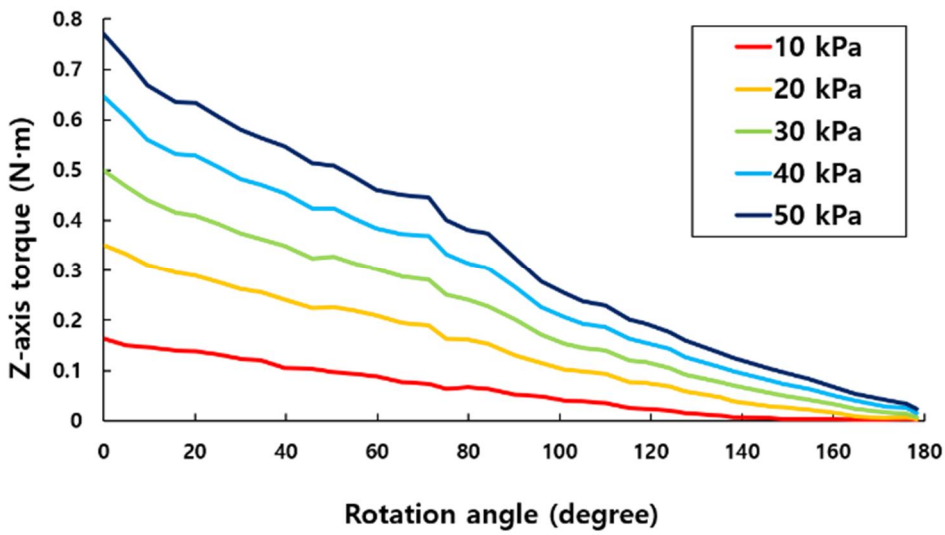

Figure. 14. Result of the experiment of the forearm rehabilitation device: Torque vs. rotation angle with varied pressure levels

The trajectory was planned at a rate of 360°/min. To reach the target angle, the two actuators have to reach the force equilibrium. From the result of the previous experiment, the force decreases nonlinearly as the rotation angle increases. If the rotation angle of the first actuator is determined, the rotation angle of the other actuator could be obtained by subtracting the angle of the first actuator from 180°. Then, different air pressures are supplied to the actuators to reach the force equilibrium.

For closed-loop, circular red and green circle markers were placed on the thumb and the little finger of the arm model respectively. The sampling rate of the vision data was about 6 Hz. The MATLAB recognized the two circle markers as points and measured the angle between the horizontal line and the line made by connecting the two marker points. Proportional control was employed for simplicity in this stage.

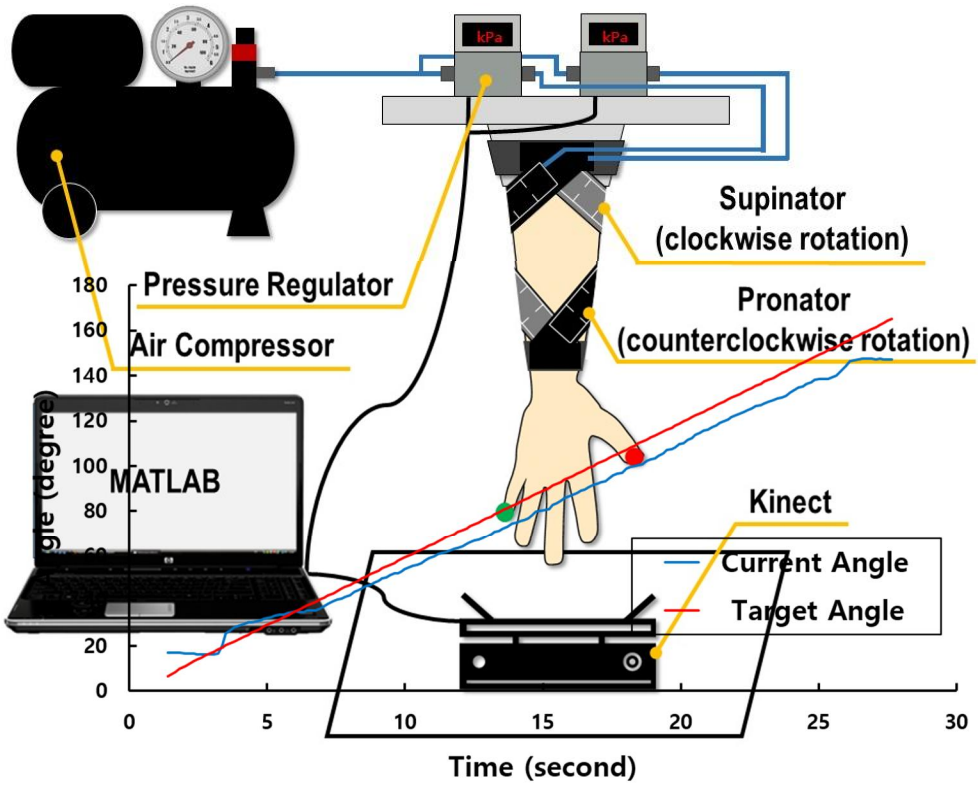

Figure. 15. Experimental setup for closed-loop control using vision system

Figure. 16. Result of closed-loop angle control of the arm model with the wearable device

The result shows that the arm model was able to follow the desired angle. From 40° to 140°, the root-mean-square error (RMSE) between the desired angle and the controlled angle was about 7.83°. A small proportional gain was set in order to avoid oscillation in this experiment. The result shows that the controlled angle followed the desired angle in general. However, relatively large errors were shown in the low and the high angle ranges (0°-

40° and 140°−180°). When the actuator fully contracted, the actuator generated a weak torque that could be overcome by the torque of the opposite actuator with little input air pressure. Considering this problem, the length of the actuator should be longer. Since the experimental setup is symmetrical, the opposite direction control can be also carried out in the same way.

4.2. Hand rehabilitation device

4.2.1. Characterization

Experiment for the characterization of a single pneumatic actuator was conducted to obtain the relationship between the rotation angle of a joint and the air pressure in the actuator. The finger model with one joint was fixed on the ground (Fig. 17). The size of the finger model is 20 mm width × 20 mm height. The torque between the motor and the finger model 1 was measured as the rotation angle decreases from 90° (finger flexion) to 0° (finger extension). The end of the actuator is fixed on the finger model 2 and can slide in the chamber of the glove like the proposed prototype.

The result shows that the highest torque was produced at a finger flexion state (Fig. 18). This results imply that low pressure should be supplied into the actuator in advance to avoid injury. The gap between two close lines decreases as the pressure increases like the results of the previous experiments. The curvature of the graph was induced by the friction between the actuator and the glove. However, the maximum torque of the device is relatively low since flexion torque values of stroke patients range from 0.5 Nm to 4 Nm [39], [40]. Therefore, the feasibility test was carried out and the result is described in the next section.

Figure. 17. Experimental setup for characterization of the pneumatic actuator for extending finger. C, D, and F rotate together and G and E are fixed on the ground in the side view.

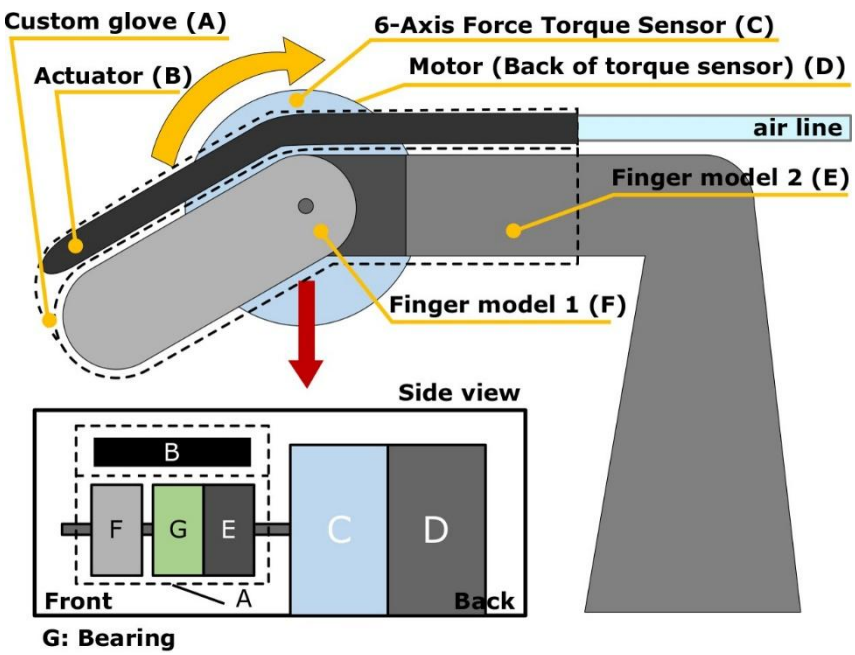

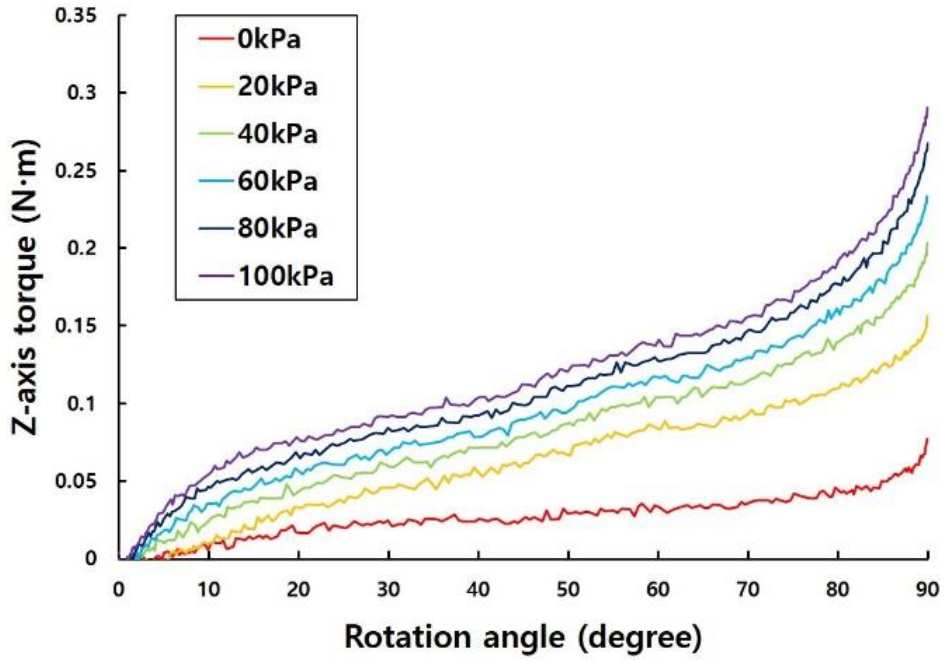

Figure. 18. Result of the experiment of the hand rehabilitation device: Torque vs. rotation angle with varied pressure levels

4.2.2. Finger extension experiment

Twelve male subjects without disabilities participated in the test. The test was designed to measure air pressure in an actuator and sensor data of a flex sensor. At the beginning of the experiment, subjects were seated with laying their left arm and hand on the table. Then, subjects wore the glove. Subjects were instructed to close their hand and relax. Air pressure was supplied into the device and increased from 0 kPa to 100 kPa for 20 seconds. After three tests were carried out, five trials were conducted as air pressure and sensor data were measured.

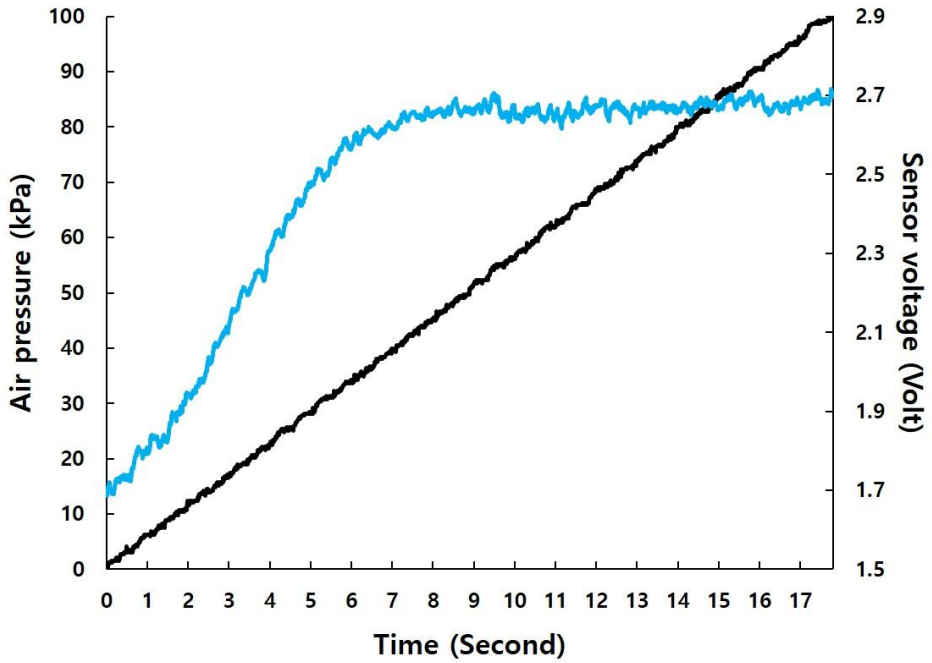

Figure. 19. Result of finger extension experiment from one of trials

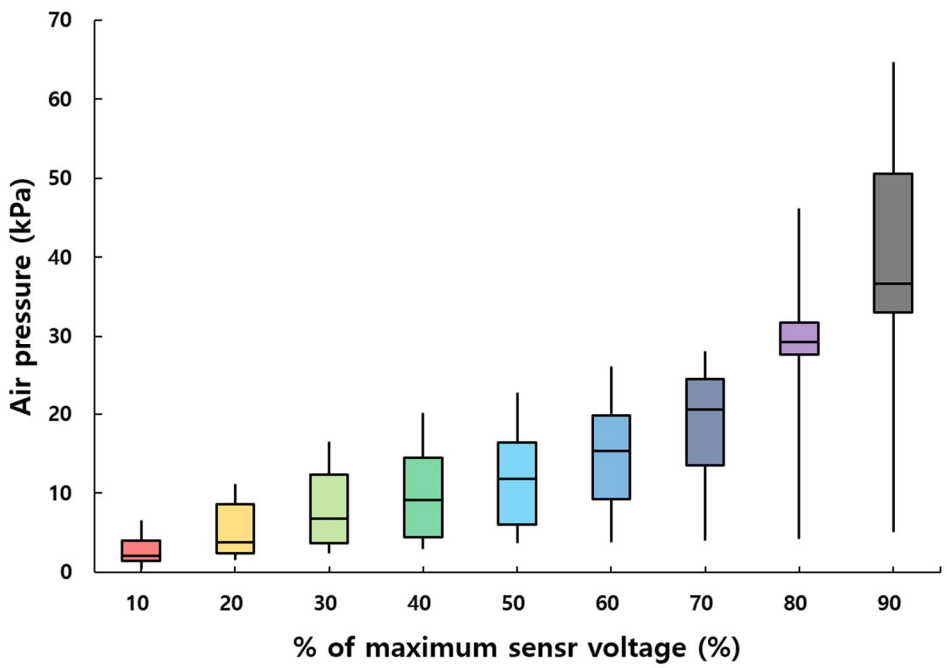

from one of subjects without disability.

Figure. 20. Box and whisker plot of finger extension experiments on

twelve male subjects without disabilities

The result from the experiment with one of the subjects shows that sensor value increases steeply until the saturation when fingers are fully extended (Fig. 19). We identify this saturation position as fully open finger position. Most of subjects show the similar trend. The average air pressures were obtained from three trials of the same subject at different percent of maximum sensor voltage. The box and whisker plot displays the five-number summary of a set of collected data voltage (Fig. 20). The minimum, first quartile, median, third quartile, and maximum air pressure were provided to achieve 0% to 90% of the maximum sensor. Median air pressure to achieve 90% of the maximum sensor value is approximately 37kPa. Although this level of air pressure must increase as the severity of the muscle stiffness increases, the result shows the possibility of utilizing this device for rehabilitation. Also, two tests on mild stroke patients prove that the device can provide enough torque to open mild paralysis patients' fingers.

Chapter 5. Conclusion

In this work, we propose soft wearable robotic devices made of lightweight fabric inflatable structures, whose design was inspired by the human musculoskeletal system. For robustness and safety, a custom-designed three-axis heat sealing system was built, and its parameters for reliable fabrication were found. In order to verify the feasibility of the devices, experiments on characterization, control, and tests with subjects were conducted. Since the devices have the advantages of compliance, safety, cost efficiency, and lightweight, the devices are expected to be used as an alternative to existing heavy and expensive rehabilitation devices.

Although silicone pads and high friction material were currently chosen for the forearm wearable device, the device often slipped on the skin when a high air pressure was supplied. To address this issue and improve the wearability, clothing techniques, such as wrist guards and elbow supports, will be employed for easy anchoring to the human body in the future. Also, experiments of the proposed devices with severe patients are required since the experiments were conducted only with the arm and finger models and subjects with mild paralysis. Effects of the proposed devices on the rehabilitation should be further investigated.

Bibliography

[1] B. Morrey, L. Askew, E. Chaoet al., "A biomechanical study of normal functional elbow motion," J Bone Joint Surg Am, vol. 63, no. 6, pp.872–7, 1981

[2] S. Hesse, G. Schulte-Tigges, M. Konrad, A. Bardeleben, and C. Werner, "Robot-assisted arm trainer for the passive and active practice of bilateral forearm and wrist movements in hemiparetic subjects," Archives of Physical Medicine and Rehabilitation, vol. 84,no. 6, pp. 915–920, 2003.

[3] D. X. Cifu and D. G. Stewart, "Factors affecting functional outcome after stroke: a critical review of rehabilitation interventions," Archives of physical medicine and rehabilitation, vol. 80, no. 5, pp. S35–S39, 1999.

[4] A. C. Lo, P. D. Guarino, L. G. Richards, J. K. Haselkorn, G. F. Wittenberg, D. G. Federman, R. J. Ringer, T. H. Wagner, H. I. Krebs,B. T. Volpeet al., "Robot-assisted therapy for long-term upper-limb impairment after stroke," New England Journal of Medicine, vol. 362, no. 19, pp. 1772–1783, 2010.

[5] O. Lambercy, L. Dovat, H. Yun, S. K. Wee, C. Kuah, K. Chua,R. Gassert, T. Milner, C. L. Teo, and E. Burdet, "Rehabilitation of grasping and forearm pronation/supination with the haptic knob," in Rehabilitation Robotics, 2009. ICORR 2009. IEEE International Conference on. IEEE, 2009, pp. 22–27.

[6] D. Andreasen, A. Aviles, S. Allen, R. Guthrie, B. Jennings, and S.

Sprigle, “Exoskeleton for forearm pronation and supination re-habilitation,” in Engineering in Medicine and Biology Society, 2004.IEMBS’04. 26th Annual International Conference of the IEEE, vol. 1. IEEE, 2004, pp. 2714-2717.

[7] E. Rashedi, A. Mirbagheri, B. Taheri, F. Farahmand, G. Vossoughi, and M. Parnianpour, “Design and development of a hand robotic rehabilitation device for post stroke patients,” in Engineering in Medicine and Biology Society, 2009. EMBC 2009. Annual International Conference of the IEEE. IEEE, 2009, pp. 5026-5029.

[8] S. Ito, H. Kawasaki, Y. Ishigure, M. Natsume, T. Mouri, and Y. Nishi-moto, “A design of fine motion assist equipment for disabled hand in robotic rehabilitation system,” Journal of the Franklin Institute, vol.348, no. 1, pp. 79-89, 2011.

[9] H. S. Lo and S. Q. Xie, “Exoskeleton robots for upper limb rehabilitation: State of the art and future prospects,” Medical Engineering & Physics, vol. 34, no. 3, pp. 261-268, 2012.

[10] S. Kyeong, G. M. Gu, and J. Kim, “Development of a portable forearm mirror image rehabilitation device,” in Ubiquitous Robots and Ambient Intelligence (URAI), 2015 12th International Conference on. IEEE, 2015, pp. 417-418.

[11] P. Maciejasz, J. Eschweiler, K. Gerlach-Hahn, A. Jansen-Troy, and S. Leonhardt, “A survey on robotic devices for upper limb rehabilitation,” Journal of neuro engineering and rehabilitation, vol. 11, no. 1, p. 3, 2014.

[12] N. Jarrass´e and G. Morel, “Connecting a human limb to an exoskeleton,” IEEE Transactions on Robotics, vol. 28, no. 3, pp. 697–709, 2011.

[13] S.−S. Yun, B. B. Kang, and K.−J. Cho, “Exo−glove pm: an easily customizable modularized pneumatic assistive glove,” IEEE Robotics and Automation Letters, vol. 2, no. 3, pp. 1725–1732, 2017.

[14] Y.−L. Park, B.−r. Chen, N. O. P ´ erez−Arancibia, D. Young, L. Stirling, R. J. Wood, E. C. Goldfield, and R. Nagpal, “Design and control of a bioinspired soft wearable robotic device for ankle–foot rehabilitation,” Bioinspiration & Biomimetics, vol. 9, no. 1, p. 016007, 2014.

[15] V. Oguntosin, W. S. Harwin, S. Kawamura, S. J. Nasuto, and Y. Hayashi, “Development of a wearable assistive soft robotic device for elbow rehabilitation,” in Rehabilitation Robotics (ICORR), 2015 IEEE International Conference on. IEEE, 2015, pp. 747–752.

[16] J. Realmuto and T. Sanger, “A robotic forearm orthosis using soft fabric−based helical actuators,” in 2019 2nd IEEE International Conference on Soft Robotics (RoboSoft). IEEE, 2019, pp. 591–59.

[17] N. W. Bartlett, V. Lyau, W. A. Raiford, D. Holland, J. B. Gafford, T. D. Ellis, and C. J. Walsh, “A soft robotic orthosis for wrist rehabilitation,” Journal of Medical Devices, vol. 9, no. 3, p. 030918, 2015.

[18] H. K. Yap, J. H. Lim, J. C. H. Goh, and C.−H. Yeow, “Design of a soft robotic glove for hand rehabilitation of stroke patients with clenched fist deformity using inflatable plastic actuators,” Journal of

Medical Devices, vol. 10, no. 4, p. 044504, 2016

[19] L. Connelly, Y. Jia, M. L. Toro, M. E. Stoykov, R. V. Kenyon, and D. G. Kamper, "A pneumatic glove and immersive virtual reality environment for hand rehabilitative training after stroke," IEEE Transactions on Neural Systems and Rehabilitation Engineering, vol. 18, no. 5, pp. 551–559, 2010

[20] R. Niiyama, X. Sun, C. Sung, B. An, D. Rus, and S. Kim, "Pouch motors: Printable soft actuators integrated with computational design," Soft Robotics, vol. 2, no. 2, pp. 59–70, 2015.

[21] J. Wirekoh and Y.–L. Park, "Design of flat pneumatic artificial muscles," Smart Materials and Structures, vol. 26, no. 3, p. 035009, 2017.

[22] H. Shaaban, C. Pereira, R. Williams, and V. Lees, "The effect of elbow position on the range of supination and pronation of the forearm," Journal of Hand Surgery (European Volume), vol. 33, no. 1, pp. 3–8,2008.

[23] R. Niiyama, C. Rognon, and Y. Kuniyoshi, "Printable pneumatic artificial muscles for anatomy–based humanoid robots," in Humanoid Robots (Humanoids), 2015 IEEE–RAS 15th International Conference on. IEEE, 2015, pp. 401–406.

[24] L. Rosenstein, A. L. Ridgel, A. Thota, B. Samame, and J. L. Alberts, "Effects of combined robotic therapy and repetitive–task practice on upper–extremity function in a patient with chronic stroke," American Journal of Occupational Therapy, vol. 62, no. 1, pp. 28–35, 2008.

[25] C. Thevenin-Lemoine, P. Denormandie, A. Schnitzler, C. Lautridou, Y. Allieu, and F. Genˆet, "Flexor origin slide for contracture of spastic finger flexor muscles: a retrospective study," JBJS, vol. 95, no. 5, pp.446–453, 2013.

[26] A. E. Hines, P. E. Crago, and C. Billian, "Hand opening by electrical stimulation in patients with spastic hemiplegia," IEEE Transactions on Rehabilitation Engineering, vol. 3, no. 2, pp. 193–205, 1995.

[27] M. F. Rotella, K. E. Reuther, C. L. Hofmann, E. B. Hage, and B. F.BuSha, "An orthotic hand-assistive exoskeleton for actuated pinch and grasp," in 2009 IEEE 35th Annual Northeast Bioengineering Conference. IEEE, 2009, pp. 1–2.

[28] L. Martinez, O. Olaloye, M. Talarico, S. Shah, R. Arends, and B. BuSha, "A power-assisted exoskeleton optimized for pinching and grasping motions," in Proceedings of the 2010 IEEE 36th Annual Northeast Bioengineering Conference (NEBEC). IEEE, 2010, pp.1–2.

[29] T. Worsnopp, M. Peshkin, J. Colgate, and D. Kamper, "An actuated finger exoskeleton for hand rehabilitation following stroke," in 2007 IEEE 10th international conference on rehabilitation robotics. IEEE, pp. 896–901, 2007.

[30] M. Xiloyannis, L. Cappello, K. D. Binh, C. W. Antuvan, and L. Masia, "Preliminary design and control of a soft exosuit for assisting elbow movements and hand grasping in activities of daily living," Journal of rehabilitation and assistive technologies engineering, vol. 4, p.2055668316680315, 2017.

[31] H. In, B. B. Kang, M. Sin, and K.-J. Cho, "Exo-glove: A wearable robot for the hand with a soft tendon routing system," IEEE Robotics & Automation Magazine, vol. 22, no. 1, pp. 97–105, 2015.

[32] D. Popov, I. Gaponov, and J.-H. Ryu, "Portable exoskeleton glove with soft structure for hand assistance in activities of daily living," IEEE/ASME Transactions on Mechatronics, vol. 22, no. 2, pp. 865–875, 2016.

[33] H. K. Yap, J. H. Lim, F. Nasrallah, J. C. Goh, and R. C. Yeow, "A soft exoskeleton for hand assistive and rehabilitation application using pneumatic actuators with variable stiffness," in 2015 IEEE international conference on robotics and automation (ICRA). IEEE, 2015, pp. 4967–4972.

[34] H. K. Yap, J. H. Lim, F. Nasrallah, and C.-H. Yeow, "Design and preliminary feasibility study of a soft robotic glove for hand function assistance in stroke survivors," Frontiers in neuroscience, vol. 11, p.547, 2017.

[35] K. C. Galloway, P. Polygerinos, C. J. Walsh, and R. J. Wood, "Mechanically programmable bend radius for fiber-reinforced soft actuators," in 2013 16th International Conference on Advanced Robotics (ICAR). IEEE, 2013, pp. 1–6.

[36] J. Ou, M. Skouras, N. Vlavianos, F. Heibeck, C.-Y. Cheng, J. Peters, and H. Ishii, "aeromorph-heat-sealing inflatable shapechange materials for interaction design," in Proceedings of the 29th Annual Symposium on User Interface Software and

Technology. ACM, 2016, pp. 121–132.

[37] G. S. Peace, Taguchi methods: a hands–on approach. Reading, MA:Addison–Wesley.

[38] J. Matsuoka, R. A. Berger, L. J. Berglund, and K.–N. An, “An analysis of symmetry of torque strength of the forearm under resisted forearm rotation in normal subjects,” The Journal of hand surgery, vol. 31, no. 5, pp. 801–805, 2006.

[39] D. G. Kamper and W. Z. Rymer, “Quantitative features of the stretch response of extrinsic finger muscles in hemiparetic stroke,” Muscle & Nerve: Official Journal of the American Association of Electrodiagnostic Medicine, vol. 23, no. 6, pp. 954–961, 2000.

[40] D. Kamper and W. Z. Rymer, “Impairment of voluntary control of finger motion following stroke: role of inappropriate muscle coactivation,” Muscle & Nerve: Official Journal of the American Association of Electrodiagnostic Medicine, vol. 24, no. 5, pp. 673–681, 2001.

Abstract in Korean

뇌졸중, 척수 손상, 외상성 뇌손상, 척수손상과 같은 다양한 원인들로 인하여 마비환자들이 존재한다. 그 중에서도 손과 팔이 마비된 환자들은 일상 생활에 어려움을 겪고 있으며, 회복을 위한 재활 훈련은 무엇보다 중요하다. 그러나 기존 재활기기들은 부피가 크고, 무거우며, 가격이 높기 때문에 환자들이 재활기기를 사용하기 위해서는 병원에 통원해야 한다는 문제가 있다. 본 논문에서는 생체 모사 디자인을 이용한 재활을 위한 공압 웨어러블 기기 개발들을 제안한다. 두 가지 기기의 주요 작동 메커니즘이 공압 팽창 방식이기 때문에, 재활기기가 경량이며, 안전하고, 부드럽다는 장점을 가지고 있다. 장치의 액추에이터가 팽창되면 액추에이터의 패턴 모양에 따라 근육과 같이 수축 동작을 도와주거나 관절을 펴주는 동작을 도와준다. 이 액추에이터의 배치에 따라 재활기기가 팔의 내전과 외전 또는 손가락을 펼치는 동작을 도와준다. 액추에이터는 자체 제작한 열 접착 CNC기기로 쉽게 제작될 수 있으며, 견실한 제작을 위해 다구치 방법(Taguchi Method)을 이용하여 매개변수를 선정하였다. 기존의 의복 소재와 결합이 가능한 소재를 이용하여 착용성을 높였으며 쉽게 교체가 가능한 형태로 개발되었다. 재활기기 특성화를 위해 팔과 손가락 모형 위에 착용시켜 관절의 각도와 압력 정도에 따라 발생하는 토크를 측정하였다. 마지막으로 재활기기의 상용 가능성을 확인하기 위해, 팔 재활기기의 경우 비전 피드백(Vision feedback)을 사용하여 팔 모형을 원하는 속도로 회전시키는 실험을 수행하였다. 손 재활기기의 경우 장애가 없는 피험자들을 대상으로 압력에 따른 굽힘 센서 값 변화를 측정하여 상용 가능성을 확인하였다.